RAPID COMMUNICATIONS

PHYSICAL REVIEW B VOLUME 46, NUMBER 18 1 NOVEMBER 1992-II

Strain-engineered incommensurability in epitaxial Heisenberg antiferromagnets

T. M. Giebultowicz,* N. Samarth,† H. Luo, J. K. Furdyna, and P. Klosowski*
Department of Physics, University of Notre Dame, Notre Dame, Indiana 46556

J. J. Rhyne
University of Missouri Research Reactor, Columbia, Missouri 75211
and National Institute of Standards and Technology, Gaithersburg, Maryland 20899
(Received 26 July 1992)

Neutron-diffraction studies of ZnTe/MnSe strained-layer superlattices show the formation of an incommensurate helimagnetic phase below 70 K. The incommensurate ordering is characterized by a wave vector that can be tuned by both strain and dimensionality. Furthermore, the incommensurate helical pitch varies smoothly with temperature, without locking in at any commensurate values.

Epitaxially layered magnetic systems fabricated using vacuum deposition techniques such as molecular-beam epitaxy (MBE) continue to attract interest because they allow the manipulation of magnetic properties through a systematic control of parameters such as dimensionality,[1,2] strain,[3] and interlayer interactions.[4] Among the wide variety of different magnetic multilayers fabricated so far, magnetic semiconductor (MS) superlattices occupy a unique niche as examples of frustrated multilayer Heisenberg antiferromagnets[3] and spin glasses[1] dominated by short-ranged exchange. While magneto-optical phenomena in MS superlattices have been investigated in great detail in recent years,[5,6] the magnetic properties of these systems have only just begun to be understood.

For example, thin MnSe layers stabilized in strained-layer superlattices such as ZnSe/MnSe provide a model system in which to study the effects of strain and dimensionality on a face-centered-cubic (fcc) Heisenberg antiferromagnet. The fcc Heisenberg antiferromagnet itself is a problem that continues to attract contemporary interest[7] despite several decades of study.[8] Recent neutron-diffraction studies of ZnSe/MnSe superlattices[3] have shown that the MnSe layers exhibit a continuous phase transition to a *commensurate* antiferromagnetic phase characterized by a type-III tetragonal magnetic unit cell.[9] The in-plane compressive strain experienced by the MnSe layers results in the stabilization of a single-domain type-III order in which the tetragonal axis of the magnetic unit cell is parallel to the growth direction. In this paper, we show how one can dramatically alter the magnetic behavior of such layered antiferromagnets by simply modifying the strain configuration in which they are placed. We find that if MnSe layers are subject to in-plane *tensile* strain instead of compressive strain, the system is driven into an *incommensurate* helimagnetic phase that exhibits at least two qualitatively new aspects: first, that in-plane tensile strain can induce incommensurate helical states in a system which is a commensurate antiferromagnet under unstrained and in-plane compressive strain conditions; second, that the incommensurability of the ordered phase can be "tuned" by changing the strain and the dimensionality (thickness) of the magnetic layers.

Modulated magnetic structures that are incommensurate (IC) (or high-order commensurable) with the underlying crystalline lattice have been known for several decades,[10,11] and are still the focus of substantial theoretical[12] and experimental[13] interest, because of predictions of new universality classes. However, as pointed out recently,[12] much of the experimental data giving the temperature variation of the incommensurability as well as the critical exponents are still not understood. It is hence important to identify new classes of systems in which incommensurate phases may be found—particularly those that may be easy to model theoretically. IC magnetism typically arises from competing ferromagnetic and antiferromagnetic interactions or is the result of anisotropic spin-orbit interactions. In any case, the properties that lead to IC behavior are usually a "given" for a particular material and cannot be continuously tuned. The system described in our study represents a different class of magnetism in which the magnetic phase of a material can be artifically tuned through "strain-engineering" to exhibit either commensurate behavior or incommensurate behavior. The ability to vary the magnetic layer thickness also allows the study of finite-size effects on the incommensurability exhibited by the system.

We focus here on ZnTe/MnSe superlattices in which strained zinc-blende layers of MnSe are sandwiched between nonmagnetic layers of ZnTe. The nonmagnetic layers are thick enough that the MnSe layers are magnetically isolated; the only reason to use a superlattice structure is to provide enough magnetic material for the experimental measurements. The magnetic layers in these strained ZnTe/MnSe superlattices are subject to an in-plane tensile strain and a perpendicular compression since the unstrained lattice parameters of the ZnTe and MnSe are 6.099 Å and 5.92 Å, respectively. As the in-plane lattice parameters match up, the MnSe parameter in the growth direction shortens to diminish the change in the unit-cell volume. The superlattices used in this study are grown by MBE on (001) GaAs wafers (typically, 2–3 cm^2 in area) at a substrate temperature of 320 °C, after first depositing a 2-μm buffer layer of ZnTe. The structure of the samples studied is described by the

TABLE I. Diffraction data from ZnTe/MnSe samples.

Sample No.	ZnTe layer thickness (in monolayers)	MnSe layer thickness (in monolayers)	$-\gamma=1-c/a$	Λ/a
1	23	17	0.0625±0.0005	3.42±0.01
2	19	13	0.0615±0.0005	3.21±0.01
3	17	10	0.0595±0.0005	2.92±0.01
4	28	10	0.0675±0.0005	3.26±0.01

specific parameters listed in Table I. We will refer to the growth direction as [001]. The sample surface is monitored during growth by *in situ* reflection high-energy electron diffraction (RHEED) at 10 keV. By monitoring oscillations in the intensity of the specular spot in the RHEED pattern along the [011] azimuth, superlattice periods can be precisely timed in integral numbers of monolayers.

Neutron-diffraction experiments are performed at the 20-MW reactor at the National Institute of Standards and Technology using a triple-axis spectrometer operated in the elastic diffraction mode, with a pyrolitic graphite (PG) monochromator and analyzer, and with a 5-cm PG filter in the incident beam. The energy of the incident neutron beam is 14.8 meV, and the angular collimation is 40′ throughout. Scans along the [001] direction in the vicinity of Bragg reflection positions for bulk unstrained materials produce characteristic diffraction patterns from the superlattice crystal structure, with harmonic peaks occurring at regular intervals $2\pi/L$ in Q-space (where L is the bilayer thickness). The period L determined from these peaks is in very good agreement with that expected from RHEED oscillations. The superlattice reflections show only a slight broadening, and their deconvoluted widths indicate that the range of crystalline coherence in the samples in the growth direction as well as in the growth plane is >1000 Å. From a straightforward analysis of nuclear diffraction data, we are able to measure both the in-plane and out-of-plane lattice parameters (a and c, respectively) of the strained MnSe layers. This analysis is summarized in Table I, where we represent the lattice distortion in terms of the distortion parameter γ, which is defined as $\gamma=(c/a-1)$. Table I shows that the lattice distortion changes from sample to sample depending on the ratio of the MnSe to ZnTe thickness.

At low temperatures, diffraction scans in the (010) and (001) planes in Q-space reveal distinct maxima at $(\pm\delta,0,l),(2\pm\delta,0,l),\ldots$ (where l is an odd integer), and at $(1\pm\delta,l,0),(3\pm\delta,l,0),\ldots$, and symmetry equivalent pairs (Fig. 1). The temperature behavior of these peaks and their Q dependence clearly indicate their magnetic origin. Namely, these peaks only appear below a characteristic Néel temperature (typically around 70 K) and increase in intensity as the temperature is further lowered. Measurements at larger values of Q show the characteristic suppressing of intensity by the magnetic form factor $f(Q)$. The relative intensities of various (hkl) reflections allows us to deduce that the spin directions are confined to the (100)-type planes perpendicular to the multilayer plane. The peaks are clearly shifted from low-order commensurate lattice positions [e.g., $(\frac{2}{3},1,0)$] and the incommensurate helimagnetic structure deduced from the diffraction data is shown in Fig. 2. Two equivalent helical domains exist, directed along the [010] and [100] directions. The deconvoluted widths of scans along [010] and [100] indicate that the helical order is long ranged (>1000 Å) within the layer plane, while scans parallel to the growth direction show the order in that direction to be essentially limited by the layer thickness. Hence, the helical domains consist of (100) [or (010)] "bands" of antiferromagnetically coupled spins, with the direction of the spins rotating by an angle φ for successive bands as shown in Fig. 2.

The reflection index δ is related to the angle φ and the helix period Λ through $\delta=\varphi/\pi=a/\Lambda$. Note that for

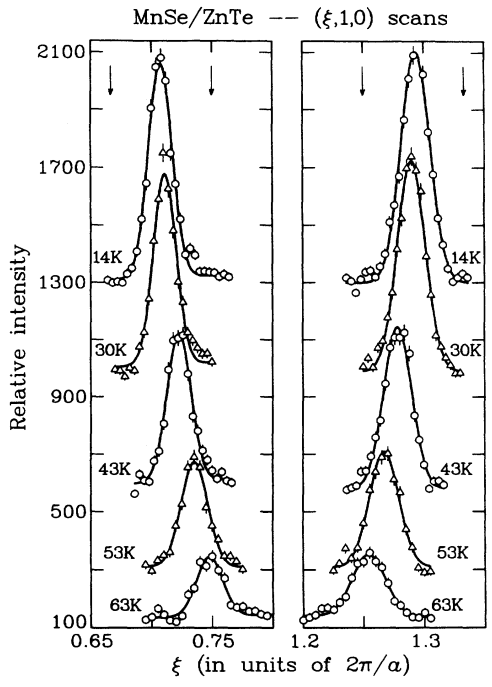

FIG. 1. Neutron-diffraction scans for a ZnTe/MnSe superlattice along the $(\xi,1,0)$ line in Q-space showing pairs of magnetic reflections at $(1\pm\delta,1,0)$ for different temperatures below the Néel temperature. The reflections correspond to incommensurate helical order, with a period Λ given by $\delta=a/\Lambda$. The vertical arrows show the peak positions corresponding to commensurate helices with $\Lambda=3a$ and $4a$. The signal was counted against a fixed incident-beam monitor rate, and the counting time per data point was approximately 4 min.

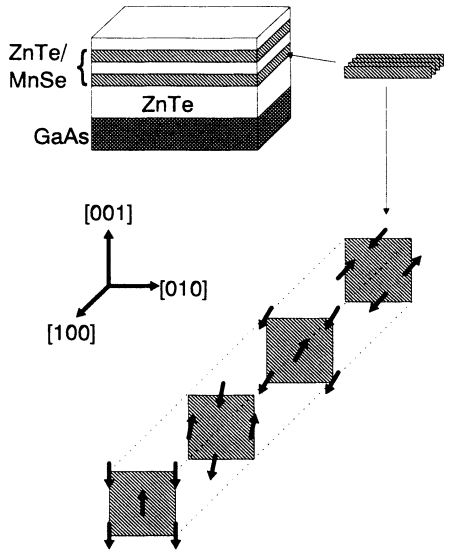

FIG. 2. Helimagnetic structure deduced from the scans in Fig. 1. Note that the helical axis is oriented along [100] (or equivalently [010]) and hence lies within the epitaxial layer plane. Since the magnetic order is limited by the MnSe layer thickness in the growth direction ([001]) but is long ranged along [010] and [100], we obtain (100) and (010) "bands" of antiferromagnetically ordered spins, with the spins on adjacent bands rotating by an angle φ about the helix axis. For $\varphi=0$, the structure is identical to the well-known type-I ordering, while for $\varphi=90$, we obtain the so-called "Keffer" structure.

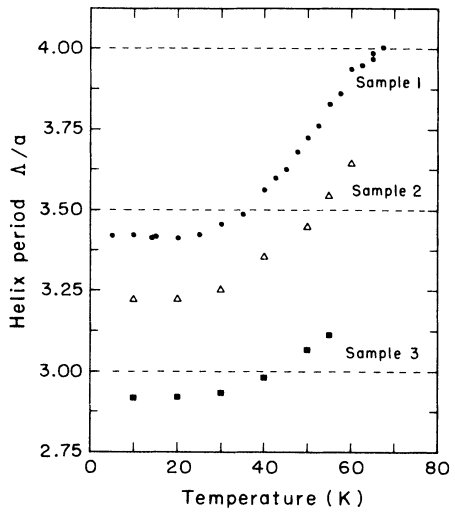

FIG. 3. Temperature dependence of the incommensurate helix period for three different ZnTe/MnSe superlattices. The dashed lines correspond to low-order commensurable periods, showing that there is no tendency to lock-in at such values of the helix period.

$\varphi=0$, which corresponds to a helix with an infinite period, this order is identical to the well-known collinear type-I structure,[9] while for $\varphi=90°$ (i.e., $\Lambda=2a$), the helical structure becomes identical with the canted type-III order which is usually referred to as the Keffer structure.[14] In all the samples studied in this paper, the angle φ lies in the range between 45° and 62°, and does not show any tendency to lock in at values corresponding to low-order commensurable order. As the temperature is lowered from the Néel temperature, the helix period decreases and then saturates below around $T=20$ K (Fig. 3). The saturation values of the modulation period for each sample expressed in reduced units ($\Lambda/a=\pi/\varphi$) are given in Table I. This table clearly shows that the incommensurable helix period is a function of both the strain and the thickness (or dimensionality) of the magnetic layers.

The above results may be understood to a first approximation using a simple energy-minimizing argument to determine the zero-temperature magnetic order for the strained MnSe layers. The low-temperature saturation value of the helix period may then be related to parameters such as layer thickness and tetragonal distortion. The temperature dependence of the helical modulation requires a more sophisticated theoretical treatment and will not be addressed in the present paper.

We assume that the tetragonal distortion of the MnSe layers leads to different exchange interactions parallel to the growth direction. Let J_1 and J_2 denote the antiferromagnetic (AF) nearest-neighbor (NN) and next-nearest-neighbor (NNN) exchange integrals, respectively, for an *undistorted* MnSe lattice. The NN exchange constants parallel and perpendicular to the growth direction for a *strained* lattice, are denoted by $J_{1\parallel}$ and $J_{1\perp}$, respectively. In a first approximation, we neglect the anisotropy in the NNN coupling. The strain configuration of interest to us is that in which $c/a<1$. Since the out-of-phase NN's are closer than those in-plane, it is reasonable to assume that $J_{1\perp}>J_{1\parallel}$. The total magnetic energy per spin for a strained MnSe layer of finite thickness in the helimagnetic state shown in Fig. 1 is then

$$U(\varphi)=E_0+[8\Delta J_1-(8/N)J_{1\perp}]\cos\varphi-4J_2\cos 2\varphi\ , \qquad (1)$$

where N is the number of magnetic monolayers constituting the MnSe layer, and where $\Delta J_1=J_{1\perp}-J_{1\parallel}$. The first of the right-hand terms, E_0, is the "interband" coupling energy, which is not sensitive to the stacking order of the AF planes, i.e., to the value of φ. The second term describes the energy of interactions between the spins and their neighbors located in adjacent bands. The $8J_{1\perp}/N$ arises because the spins belonging to the lowermost and the uppermost rows in each band do not have a full set of NN's, and hence directly leads to finite-size effects. Finally, the last term in Eq. (1) is the energy of interactions with the NNN's located in the second-nearest bands to a given spin.

Minimizing the energy with respect to φ, we find that for $0\le\varphi\le 90°$, the ground-state helical configuration is given by

$$\varphi|_{U=\min}=\arccos\left[\frac{\Delta J_1-(1/N)J_1}{2J_2}\right]\ . \qquad (2)$$

where we have assumed that the strain-induced anisotropy ΔJ_1 is small in comparison with the exchange integral J_1 for an undistorted system, so that $J_{1\perp}\approx J_1$. The

energy-minimizing value of φ and the minimum-energy value are both functions of the dimensionless parameter $\Delta J_1/J_2$. A straightforward analysis shows that, for $0 \leq \Delta J_1/J_2 \leq 2$, the helical configuration leads to a lower magnetic energy than the type-I or type-III order.

Finally, we attempt to relate measurements of the helical pitch as a function of lattice distortion to known exchange parameters. We assume that the exchange integral J_1 in these compounds is a *scalar* function of the ion-ion distance R, and that in the relevant range of the variation in R, $J_1(R)$ can be approximated by a linear dependence. Equation (2) can then be recast in the form

$$\varphi|_{\text{helix}} = \arccos \frac{\mathcal{J}_{1/2}}{2} \left[\frac{\gamma}{2} \frac{dj_1}{dr} - \frac{1}{N} \right], \tag{3}$$

where $\mathcal{J}_{1/2} = J_1/J_2$. The parameters $j_1 = J_1/J_1^0$ and $r_1 = R_1/R_1^0$ are the nearest-neighbor exchange and the ion-ion distance normalized to their respective values for an undistorted lattice. We now use our experimentally observed value of φ, lattice distortion parameter γ, and the number of magnetic monolayers N, to deduce values for both the ratio of the NN to NNN exchange and for the variation of the exchange integral with ion-ion distance. The self-consistency of the results obtained from such an analysis (Table II) indicates the essential correctness of our simple mean-field model. However, the value of dj_r/dr_1 obtained from our fits (≈ 9.5) is $\sim 50\%$ larger than values presented in earlier theoretical[15] and experimental work.[16,17] This disagreement probably arises because our simple model ignores the effect of the angular change in the Mn—Se—Mn bonds on the exchange integral.

TABLE II. Fit of Eq. (3) to measured data.

Sample No.	Input data N	Input data $-\gamma$	Λ/a values Fitted	Λ/a values Measured
1	17	0.0625	3.423	3.42±0.01
2	13	0.0615	3.191	3.21±0.01
3	10	0.0595	2.938	2.92±0.01
4	10	0.0675	3.271	3.26±0.01
Fitted parameter values	$dj_1/dr = 9.4$		$J_1/J_2 = \mathcal{J}_{1/2} = 5.3$	

In summary, we have shown that the magnetism in thin epitaxially grown Heisenberg antiferromagnets such as MnSe can be controlled using "strain-engineering." The observed behavior is predicted within a simple mean-field model—but a more sophisticated theoretical treatment of the problem is clearly warranted. Finally, we note that a recent phenomenological theory within the Landau-Ginzburg framework produces qualitative agreement with our experimental findings and it is anticipated that further theoretical work will help us understand the observed temperature dependence of the helical ordering.[18]

We thank U. Debska for the purification of the source materials. This work was supported by National Science Foundation Grant No. DMR-8821635 and by ONR Grant No. N-00014-90-J-1782.

*Present address: National Institute of Standards and Technology, Gaithersburg, MD 20899.

†Present address: Department of Physics, The Pennsylvania State University, University Park, PA 16802.

[1] D. D. Awschalom, J. M. Hong, L. L. Chang, and G. Grinstein, Phys. Rev. Lett. **59**, 1733 (1987).

[2] A. Gavrin, J. R. Childress, C. L. Chien, B. Martinez, and M. B. Salamon, Phys. Rev. Lett. **64**, 2438 (1990).

[3] N. Samarth, P. Klosowski, H. Luo, T. Giebultowicz, J. K. Furdyna, J. J. Rhyne, B. E. Larson, and N. Otsuka, Phys. Rev. B **44**, 4701 (1991).

[4] C. A. Ramos, D. Lederman, A. R. King, and V. Jaccarino, Phys. Rev. Lett. **65**, 4704 (1991).

[5] D. D. Awschalom, M. R. Freeman, N. Samarth, H. Luo, and J. K. Furdyna, Phys. Rev. Lett. **66**, 112 (1991), and references therein.

[6] N. Dai, H. Luo, F. C. Zhang, N. Samarth, M. Dobrowolska, and J. K. Furdyna, Phys. Rev. Lett. **67**, 3824 (1991), and references therein.

[7] A. J. Annila *et al.*, Phys. Rev. B **45**, 7772 (1992).

[8] D. ter Haar and M. Lines, Philos. Trans. R. Soc. London Ser. A **254**, 521 (1962).

[9] J. S. Smart, *Effective Field Theories of Magnetism* (Saunders, Philadelphia, 1966).

[10] P. Bak, Rep. Prog. Phys. **45**, 587 (1982).

[11] Yu. A. Izyumov, Physica B **174**, 9 (1991).

[12] W. M. Saslow, M. Gabay, and W. M. Zhang, Phys. Rev. Lett. **68**, 3627 (1992).

[13] J. Wang, D. P. Belanger, and B. D. Gaulin, Phys. Rev. Lett. **66**, 3630 (1991).

[14] F. Keffer, Phys. Rev. **126**, 896 (1962).

[15] B. E. Larson, K. C. Hass, H. Ehrenreich, and A. E. Carlsson, Phys. Rev. B **37**, 4137 (1988).

[16] J. K. Furdyna, J. Appl. Phys. **64**, R29 (1988).

[17] W. J. M. de Jonge and H. J. M. Swagten, J. Magn. Magn. Mater. **100**, 322 (1991).

[18] R. Cohen and K. E. Newman, Phys. Rev. B (to be published).